C. R. Chimie 18 (2015) 1152–1160

Contents lists available at ScienceDirect

Comptes Rendus Chimie

www.sciencedirect.com

International Symposium on Air & Water Pollution Abatement Catalysis (AWPAC) – Catalytic pollution control for stationary and mobile sources

Decolorization and mineralization of yellow 5 (E102) by UV/Fe^{2+}/H_2O_2 process. Optimization of the operational conditions by response surface methodology

Edison GilPavas [a,*], Carlos M. Gómez [a], Jacek Michal Rynkowski [b], Izabela Dobrosz-Gómez [c], Miguel Ángel Gómez-García [d]

[a] GIPAB: Grupo de Investigación en Procesos Ambientales, Departamento de Ingeniería de Procesos, Universidad EAFIT, Carrera 49 #7 sur 50, Medellín, Colombia
[b] Institute of General and Ecological Chemistry, Lodz University of Technology, 90-924 Lodz, Zeromskiego 116, Poland
[c] Grupo de Investigación en Procesos Reactivos Intensificados con Separación y Materiales Avanzados – PRISMA, Departamento de Física y Química, Facultad de Ciencias Exactas y Naturales, Universidad Nacional de Colombia, Sede Manizales, Campus La Nubia, km 9 vía al Aeropuerto la Nubia, Apartado Aéreo 127, Manizales, Caldas, Colombia
[d] Grupo de Investigación en Procesos Reactivos Intensificados con Separación y Materiales Avanzados–PRISMA, Departamento de Ingeniería Química, Facultad de Ingeniería y Arquitectura, Universidad Nacional de Colombia, Sede Manizales, Campus La Nubia, km 9 vía al Aeropuerto la Nubia, Apartado Aéreo 127, Manizales, Caldas, Colombia

ARTICLE INFO

Article history:
Received 30 November 2014
Accepted after revision 12 August 2015
Available online 19 September 2015

Keywords:
Photo-Fenton process
Tartrazine
Yellow 5
NaCl scavenging effect
Statistical optimization

ABSTRACT

In this study, the optimization and implementation of a homogeneous photo-Fenton process for the decolorization and mineralization of a wastewater containing highly concentrated yellow 5 (E102) dye, resulting from an industry placed in the suburbs of Medellin (Colombia), is presented. Response surface methodology was applied as a tool for the optimization of operational conditions such as initial dyestuff concentration, H_2O_2 concentration, and UV-radiation power (number of lamps). The decolorization, degradation and mineralization efficiencies were used as response variables. The following conditions were found to be optimal for decolorization and mineralization of yellow 5: UV radiation of 365 nm (4 W, one lamp), dye concentration of 200 mg/L, Fe^{2+} concentration of 1.0 mM, H_2O_2 concentration of 1.75 mL/L, treatment time of 180 min, Fe^{2+} concentration of 1 mM and pH = 3. Under these conditions (180 min), the photo-Fenton process allowed us to reach ca. 100% of color dye degradation, 99% of COD degradation, and 85% of mineralization (TOC). The scavenging effect of the Cl^- anion on the photodegradation process was also confirmed.

1. Introduction

Azo dyes are complex aromatic compounds characterized by both high stability and toxicity. Their practical application includes textile, pharmaceutical, cosmetic, and food industries. Their presence in wastewaters gives a strong coloration to the waterbodies, suppressing the photosynthesis processes [1]. The colorant's structures and attributes are very complex and variable. Many of them present organic origin, solubility in water, high resistance to the action of chemical agents as well as low biodegradability [2].

* Corresponding author.
E-mail address: egil@eafit.edu.co (E. GilPavas).

http://dx.doi.org/10.1016/j.crci.2015.08.001
1631-0748/

One of the most consumed pigments by the textile industry is the yellow one, originating from the diazoacetoacetanilides group. Currently, the yellow 5 dye (E102 or tartrazine; molecular formula: $C_{16}H_9N_4O_9S_2Na_3$; λ_{max} = 430 nm) is one of the most employed due to its brightness, color, and favorable price [3,4]. Since the Colombian environmental legislations have become more rigorous for these kinds of pollutants, the mineralization of residual colorants started to be a challenge for both industrial and academic research groups. In general, conventional biological treatments are useless for their degradation, basically due to the formation of secondary compounds that in turn are more toxic than their parent substances [5]. Moreover, sedimentation, flocculation, and adsorptive methods are also ineffective for their efficient remotion [6–8]. Recently, a special interest has presented the so-called advanced oxidation processes (AOPs) [8,9]. They are based on the generation of highly reactive hydroxyl radicals as primary oxidants. The main advantages of their application are: simplicity of use, accessibility, and moderate cost [10]. Among the AOPs, Fenton's and photo-Fenton's type reactions are very promising [11,12]. The pollutant oxidation using Fenton's reagent is a homogeneous oxidation that occurs in the presence of H_2O_2 and ferrous ions mixtures. In an acidic environment, if H_2O_2 is added to an aqueous system containing an organic substrate and ferrous ions, a complex redox reaction occurs.

The ferrous ion initiates and accelerates the decomposition of H_2O_2, resulting in the generation of hydroxyl radicals, $^{\bullet}OH$, a powerful oxidation agent with an oxidation potential of 2.8 V. They are able to attack rapidly the organic substrates, causing their chemical decomposition by H-subtraction and addition to C = C unsaturated bonds.

Thus, numerous competing reactions involving Fe^{2+}, Fe^{3+}, H_2O_2, $^{\bullet}OH$, $HO^{\bullet}_2$ and other radicals derived from the substrate may take place. The $^{\bullet}OH$ radicals can be scavenged by reacting with Fe^{2+} or H_2O_2, leading to the formation of Fe^{3+} and $HO^{\bullet}_2$, respectively. Thus, the formed Fe^{3+} ions can react with H_2O_2, involving $^{\bullet}OH$ and $HO^{\bullet}_2$ radicals and resulting in the regeneration of Fe^{2+} ions. According to the literature [11], the addition of UV radiation to Fenton's process, known as photo-Fenton ($H_2O_2/Fe^{2+}/UV$), appears to be an interesting option for the decolorization of dyes due to its capacity to influence the direct formation of $^{\bullet}OH$ radicals. Thus, UV radiation can accelerate the mineralization process through the following pathways:

- the enhancement of Fe^{2+} regeneration from the additional photo-reduction of Fe^{3+} species [10–12];
- the photolysis of hydrogen peroxide [13];
- the photolysis of complexes of Fe^{3+} with some oxidation products, such as oxalic acid.

This work deals with the optimization and implementation of a photo-Fenton process for the decolorization and mineralization of a wastewater containing highly concentrated yellow 5 (E102) dye, resulting from an industry placed in the suburbs of Medellin (Colombia). Since decolorization can be achieved more easily than mineralization, the effect of different process variables (the initial dyestuff concentration, H_2O_2 concentration, and the UV-radiation power [number of lamps]) on color, COD, and TOC removal efficiencies was considered. However, most of the recently published studies [14–18] concerning the effect of these variables adopt rather a one-factor-at-a-time approach (one parameter was varied thereby keeping the others constant). Nevertheless, the process parameters may involve synergistic effects, due to complex interactions between the process variables. Therefore, the application of conventional optimization techniques can be inadequate, time consuming, and does not allow a precise process optimization. In order to overcome these drawbacks, the optimization can be based on statistical design tools. Thus, the response surface methodology (RSM) was applied as a tool for the optimization of yellow 5 degradation and mineralization by a homogeneous photo-Fenton (PF) process, at laboratory scale. This method permits us to assess the individual and interactive effects of several operating parameters (the initial dyestuff concentration, H_2O_2 concentration, and the UV-radiation power [number of lamps]) on the treatment efficiency (color, COD, and TOC removal). As far as we know, no similar study was performed for the treatment of yellow 5 dye using photo-Fenton process. The RSM is a statistical technique that allows establishing the relationships between several independent variables and one or more dependent ones, reducing the number of experimental trials, experimental errors and overall cost [19,20]. The optimization of the operational conditions by the RSM involved the following steps:

- the implementation of the statistically designed experiments;
- the estimation of the coefficients of a mathematical model using regression analysis;
- the prediction of the response;
- the verification of the adequacy of the model.

Among the available statistical design methods, a multilevel Box–Behnken experimental Design (BBD) was chosen for the purpose of response optimization [21,22]. The scavenging effect of the Cl^- anion on the photodegradation process was also investigated. Therefore, the decolorization and mineralization of yellow 5 by a homogeneous UV/Fenton process was optimized by the RSM-BBD method. Considering that in the case of yellow 3 dye [23] homogeneous UV/Fenton process ($UV/Fe^{2+}/H_2O_2$) was proved to be more efficient than the heterogeneous one, more acceptable for the environment, we have decided to apply the homogeneous variation to this process. Moreover, although the heterogeneous catalysts present usually higher reactivity and a reduced dependence on the pH of the solution in comparison to the homogeneous Fe catalysts, they also have higher rates of the side reaction of hydrogen peroxide decomposition into water and oxygen [24].

2. Materials and methods

2.1. Reagents

All reagents were of analytical grade: NaCl (99%), yellow 5 colorant (98%), $FeSO_4{\cdot}7H_2O$ (99%), H_2O_2 (30%),

and H_2SO_4 (98%), furnished by Merck, and used without any further purification. The corresponding reagent solutions were prepared using extra pure water (Milli-Q system; 18.0 MΩ·cm resistivity). All studies were performed with simulated yellow 5 wastewater since the received industrial samples were mixtures of different dyes, between them yellow 5 one, with variable concentration depending on the specific industrial activities. Thus, simulated wastewater samples of yellow 5, with concentrations in the range from 200 to 1000 mg/L, were prepared by diluting the corresponding amount of the dye with deionized water. This range of concentration was selected according to the monitoring of the enterprise activity performed during one month.

2.2. Photo-reactor

A schema of the photo-Fenton process is depicted in Fig. 1. The experiments were performed at 25 °C, as described previously in details [8,21]. For each experiment, a desired quantity of reactive solution was freshly prepared. Additionally, the required amounts of $FeSO_4{\cdot}7H_2O$ and H_2O_2 were added to the obtained solution. Its pH = 3 was fixed using 1 N H_2SO_4. This pH value is highly recommended for Fenton's reaction since it avoids the formation and precipitation of Fe^{2+} salts. At the beginning of each experiment, the dye solution was fed into the reactor. Next, Fe^{2+} and H_2O_2 were charged. The UV lamp (365 nm F6T5 Black Light Hg and 4 W power) was switched on when the 1-L reactor was completely filled and the time started to be monitored. Each time, 5-mL samples were taken at periodic intervals for immediate analysis.

2.3. Analytical methods

In order to follow the efficiency of yellow 5 (E102) decolorization (%DD) and degradation (%COD), the samples were withdrawn at certain time intervals for spectrophotometric analysis (vis double-beam spectrophotometer, Spectronic Genesys 2PC), in the range from 200 to 700 nm. A calibration plot based on Beer–Lambert's law was prepared to correlate absorbance magnitude with dye concentration. The absorbance, measured at 430 nm, corresponds to the dyes' color. Its changes were used to monitor the decolorization efficiency. The changes in the absorbance measured at 246 nm, representing the aromatic part of yellow 5 (E102), indicated the degradation of the aromatic part of the dye. Standard methods [25] were used for the quantitative analysis of the chemical oxygen demand (COD), the total organic carbon (TOC). The COD analyses were performed following the closed reflux method with colorimetric measurements (method 5220D). Mineralization was monitored by changes in the total organic carbon (TOC) content. TOC measurements were carried out with a Shimadzu analyzer (model TOC-5000A), following the method 5310D. The BOD_5 measurements were performed following the respirometric method (5210B).

The efficiency of the photo-Fenton process was calculated as the dye, COD, and TOC degradation percentages (%DD, %DCOD, and %DTOC, respectively). For example, the %DD was calculated using the following expression:

$$\%DD = \frac{(C_0 - C)}{C_0} \times 100 \quad (1)$$

where C_0 and C correspond to the initial and final dye concentrations, respectively.

2.4. Experimental design and statistical analysis

The RSM was chosen and implemented to establish the influence of different operating factors on the decolorization and mineralization of yellow 5 by the photo-Fenton process. A multifactorial BBD was defined to evaluate the interactive effect of process variables and to perform its optimization. The following variables were selected for RSM: H_2O_2 concentration, initial dyestuff concentration, and UV-radiation power (number of lamps). The RSM

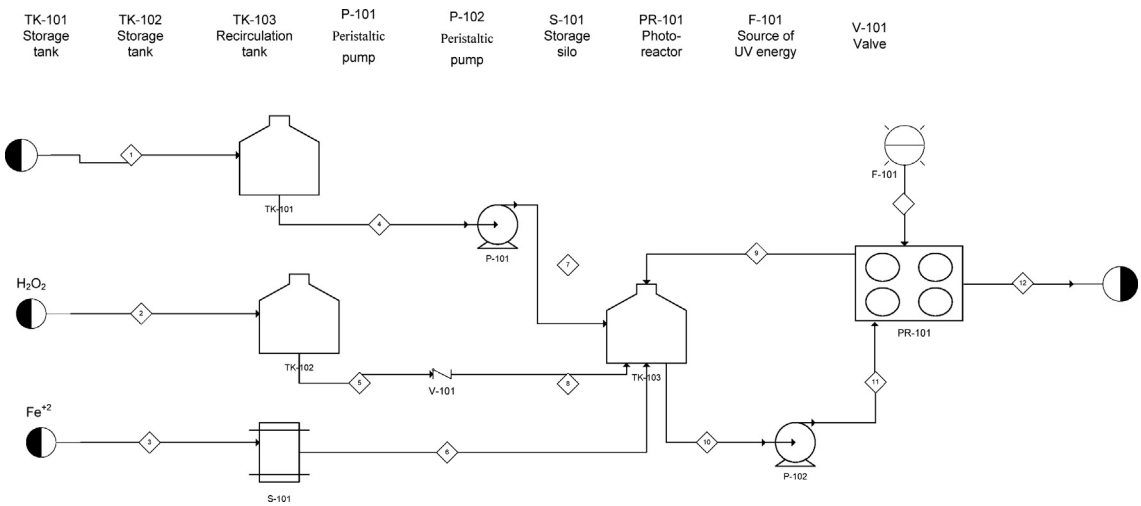

Fig. 1. Scheme of the photo-Fenton process.

coupled with BBD was chosen to find the relationship between the response functions (%DD and %COD) and variables using the statistical software tool Statgraphics 5.1 (Statistical Graphics Corp 1999–2004). The three-level second-order design demanded a relatively low number of experiments. Thus, fifteen tests with replica including three center points were randomly made in order to avoid any systematic error. From preliminary experiments (not presented here), three different levels (values) were chosen for each of the four following variables (Table 1). The interaction between the variables and the analysis of variance (ANOVA) has been studied by RSM. The quality of the fit of this model and its prediction capacity is expressed by the coefficient of determination, R^2. The variables were coded according to Eq. (2):

$$X_i = \frac{(x_i - x_{pc})}{\Delta x_i} \quad (2)$$

where X_i is the code level, x_i is the non-coded value, x_{pc} corresponds to the non-coded value at the central point, and Δx_i is the change of the value between levels [8]. For the RSM, the experimental results were adjusted to a second-order multivariable polynomial (Eq. (3)):

$$Y_i = \beta_0 + \sum_1^3 \beta_i X_i + \sum_1^3 \beta_{ii} X_{ii}^2 + \sum_1^3 \sum_1^3 \beta_{ij} X_i X_j \quad (3)$$

where Y_i was the response variable; β_0, β_i, β_{ii}, and β_{ij} were the regression coefficients that correspond to the intersect, lineal, quadratic, and interactions, respectively; and X_i and X_j are the independent variables.

3. Results and discussion

3.1. Development of the regression model equation

A set of preliminary experiments (not shown here) allowed defining the variables that considerably affect decolorization, %DD, and mineralization, %DCOD, efficiency of yellow 5 by the photo-Fenton process. Thus, dyestuff concentration, H_2O_2 concentration and UV radiation, at 365 nm (number of lamps), were chosen for optimization using RSM and BBD. To examine the combined effect of three independent process parameters on its efficiency, 15 experiments were performed. Furthermore, Fe^{2+} concentration (1 mM), pH (of 3) and UV radiation (365 nm) were kept constant. The experimental design is given in Table 2, together with the corresponding experimental data. As shown in Table 2, the removal efficiencies range from 91% to 100% for %DD and 4–75% for %DCOD.

Regression analysis was performed to fit the response function (%DCOD). The developed second-order polynomial equation represents responses as functions of dyestuff concentration (A), number of lamps (B), and H_2O_2 concentration (C). An empirical relationship between the response and the input test variables in coded units can be expressed by the following equation:

$$\%DCOD = 94,5174 - 0,110208 \times A - 10,6667 \times B + 6,22222 \times C + 0,0000617188 \times A^2 - 0,0075 \times A \times B - 0,00583333 \times A \times C + 3,125 \times B^2 + 3,33333 \times B \times C - 2,88889 \times C^2 \quad (4)$$

Equation (4) describes how %DCOD was affected by the individual variables and/or their double interactions. %DCOD was linear and also quadratic with respect to dyestuff concentration, number of lamps, and H_2O_2 concentration; and it is also quadratic with respect to dyestuff concentration, number of lamps, and H_2O_2 concentration. This indicates that there are the following interactions: dyestuff concentration–dyestuff concentration, dyestuff concentration–number of lamps, dyestuff concentration–H_2O_2 concentration, number of lamps–H_2O_2 concentration, which can affect %DCOD.

3.2. Statistical analysis of photodegradation tests (ANOVA)

For all experiments, a reaction time of three hours was established and %DCOD was chosen as the response variable. Analysis of variance, ANOVA, was employed to determine the significant main and interaction effects of factors influencing %DCOD. The ANOVA results are presented in Table 3.

Table 1
Parameter levels and physicochemical properties of the studied solution.

	Parameter	Level		
Parameters and their corresponding values for experimental design	Dyestuff concentration (mg/L)	200	600	1000
	H_2O_2 concentration (mL/L)	0.5	1	2
	UV radiation, 365 nm (number of lamps)	1	2	3
The initial physicochemical characteristics of wastewater	COD (mg/L)	303	728	1128
	TOC (mg/L)	102	224	360
	pH	2.97	3.01	3.02
	BOD_5 (mg/L)	80	–	–
	BOD_5/COD	0.264	–	–
	Conductivity (μS/cm)	373	512	943
	Density (g/mL)	1.001	1.003	1.009
	Viscosity (cP)	1.002	1.002	1.002

Table 2
Experimental results of the %DD and %DCOD for the three variables and levels.

Experiment	Dyestuff concentration (mg/L)	Number of lamps	H_2O_2 concentration (ml/L)	%DD	%DCOD
1	200	1	1.25	100	55
2	200	2	0.5	100	75
3	600	2	1.25	99	39
4	1000	1	1.25	95	14
5	200	2	2	100	50
6	600	3	2	99	16
7	600	3	0.5	96	42
8	600	1	0.5	96	43
9	600	2	1.25	98	36
10	1000	2	0.5	91	4
11	600	2	1.25	95	38
12	1000	3	1.25	95	13
13	200	3	1.25	100	53
14	600	1	2	95	15
15	1000	2	2	95	2

ANOVA consists in classifying and cross-classifying statistical results. The Fisher *F*-test, based on the ratio of the respective mean-square effect to the mean-square error, was used to evaluate the presence of a significant difference from the control's response and to calculate standard errors. The bigger the magnitude of the *F* value, more significant is the corresponding coefficient. The *P* values were used to identify experimental parameters that present a statistically significant influence on a particular response. If the *P* value is lower than 0.05, it is statistically significant at the 95% confidence level [8]. According to ANOVA results, one can see that all terms in the regression model are not equally important. Only two of them (initial dye concentration [A:Ci] and A–A interactions) presented *P* values lower than 0.05 (Table 2), which implies that they have a truthfully effect on %DCOD, with a confidence interval of 95% [8,20]. Similar results were presented elsewhere [21,26]. On the other hand, the effect of H_2O_2 concentration on %DCOD removal efficiency is not as significant (in the analyzed range). However, it can present some importance and should not be ignored.

The quality of the developed model was evaluated based on the variation coefficient (R^2) and the standard deviation value. The closer the R^2 value to unity and the lower the value of the standard deviation, more accurately the response can be predicted by the model. The R^2 value was found to be 0.9878, indicating that 98.78% of the total variation in %DCOD was attributed to the studied experimental variables. Moreover, the value of the predicted R^2 (0.9878) was in very good agreement with the value of the adjusted R^2 (0.9659). Since the R^2 value is close to unity, there is a good agreement between the experimental data and those predicted by the model. The highest %DCOD (99) and %DD (100) were reached for the following experimental conditions: Fe^{2+} concentration = 1.00 mM; H_2O_2 concentration = 1.75 mL/L; one lamp UV radiation power (wavelength = 365 nm, 4 W); and initial dye concentration = 200 mg/L. The probability plots are one of the most widely used analysis tools to identify data reliability. Therefore, Fig. 2, a normal probability plot, presents the effect of each variable on %DCOD during the photodegradation process. Again, one can see that the initial dye concentration presents the most significant effect on %DCOD.

The Pareto analysis was used to identify factors that present the greatest cumulative effect on %DCOD, and thus to screen out the less significant ones. A Pareto diagram is a series of bars whose heights reflect the frequency or impact of each factor. The bars are arranged in descending order of heights, from left to right. Therefore, the factors represented by the tall bars are relatively more significant. Here, the Pareto analysis was also carried out to determine the percentage effect of each factor, according to the following equation [19,20]:

$$P_i = \left(\frac{b_i^2}{\sum b_i^2}\right) \times 100 \quad (i \neq 0) \tag{5}$$

Thus, statistically important factors correspond to all these whose values overpass the inner vertical line (Fig. 3). The vertical line corresponds to the *t* value in the *t*-Student distribution, with a 95% confidence and for 14 degrees of freedom. Next, this value is compared with the values of each effect and interaction of the analyzed factor. The comparison defines the statistical significance of each factor in the analyzed process. Therefore, the factor that

Table 3
Analysis of variance, ANOVA, for %DCOD.

Factor	Sum of squares	Degree of freedom	Mean square	*F* value	*P* value
A: dyestuff concentration	4371.13	1	4371.13	362.75	0.000
B: number of lamps	18.0	1	18.0	1.49	0.2761
C: H_2O_2 concentration	21.125	1	21.125	1.75	0.2428
AA	360.058	1	360.058	29.88	0.0028
AB	36.0	1	36.0	2.99	0.1445
AC	12.25	1	12.25	1.02	0.3596
BB	36.0577	1	36.0577	2.99	0.1442
BC	25.0	1	25.0	2.07	0.2093
CC	9.75	1	9.75	0.81	0.4096
Error total	60.25	5	12.05		
Total (corr.)	4948.93	14			
R^2 = 98.78%					
R^2_{adj} = 96.59%					

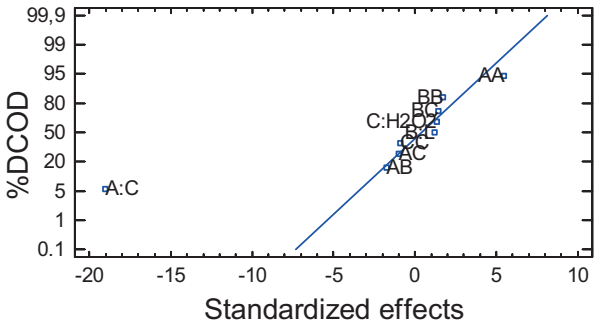

Fig. 2. Normal probability plot of the effect of the variables on %DCOD by the photo-Fenton process: A:C = initial dye concentration; B = L: UV-radiation power (number of lamps); C:PO = H_2O_2 concentration.

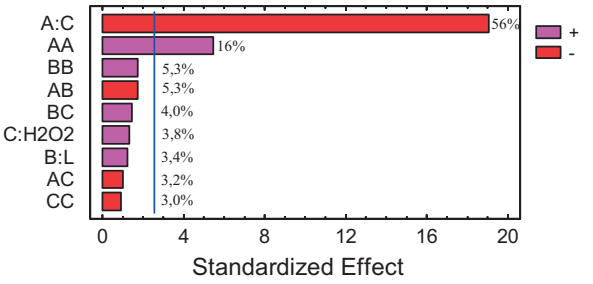

Fig. 3. (Color online.) Pareto diagram for %DCOD by photo-Fenton.

presents an influence on the degradation process is the initial dye concentration (A) and its interactions: A–A.

One can see that %DCOD is inversely proportional (−) to the initial dye concentration (A) and directly proportional (+) to the A–A interaction. Moreover, the initial dye concentration can be considered as the most dominating factor during COD degradation (Fig. 3). In fact, the higher the dye concentration is, the lower the degradation rate that can be reached (considering also that the •OH radical concentration was constant). Similar results were reported by Modirshahla et al. [13].

The surface response plot was used to study the effect of all factors on the response variable (Fig. 4). This type of plots summarizes the effect of two variables on %DCOD, considering that the third one was kept constant. One can see that %DCOD depends on the initial dye concentration (with a maximum at 200 ppm). Moreover, no significant effect of the UV-radiation power (number of lamps) on %DCOD was observed. Modirshala et al. [13] and Gupta et al. [27] reported contradictory results mainly due to differences in the reactor's configuration.

Fig. 5 shows the representative UV-vis spectra of the E102 degradation process 1.0 mM Fe^{2+} concentration. One can see that before treatment (t = 0 min), its UV-vis spectrum consists of two main characteristic absorption bands: the first one, in the UV region, with a maximum at 246 nm, corresponds to the benzenic rings of E102; and the second one, in the visible region, with a maximum at 430 nm, is a feature of the two-azo group (–N = N–), which is responsible for the bright lemon yellow dye. After 15 min of the degradation process, a significant decrease in the intensity of the absorption band in the UV region was observed. Moreover, the absorption band observed in the visible region disappears and, in its place, two new bands, at 220 and 330 nm, appear. The first band is related to the presence of unreacted and/or in situ formed H_2O_2 (by •OH) radical recombination (Eq. (6)), the second one can be attributed to the π system delocalization [28]:

$$^{\bullet}OH + {}^{\bullet}OH \rightarrow H_2O_2 \quad (6)$$

After 45 min of reaction, the band at 430 nm disappeared and the color of the solution was completely degraded. However, the other two bands (at 220 and 330 nm) still remained, indicating that some intermediate degradation compounds are reformed. It is known that the reaction intermediates (mainly oxalic and fumaric acid, highly dependent on the initial dye concentration) can be formed as a result of the oxidation of the azo dyes. Moreover, some of them are characterized by stability and toxicity much higher than these of their parent compounds [9]. Generally, up to a certain level, the higher ferrous salt concentration can generate a higher degradation rate of organic compounds. However, further addition of ferrous ions becomes inefficient, probably due to the consumption of

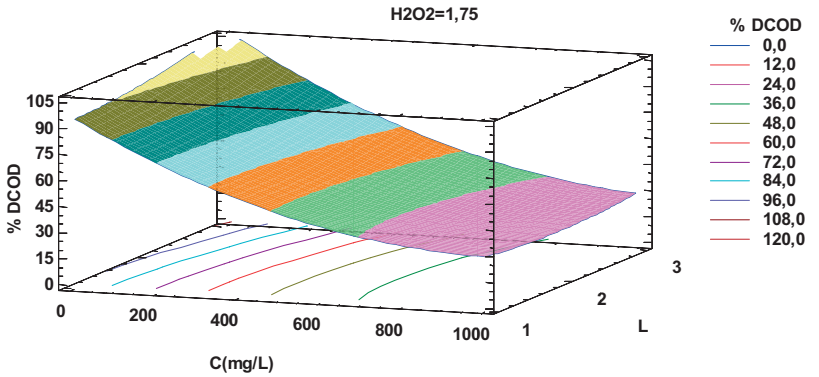

Fig. 4. (Color online.) Surface response plot of %DCOD as a function of the initial dye concentration (C) and of the UV-radiation power (number of lamps). Constant H_2O_2 dose = 1.75 mL/L.

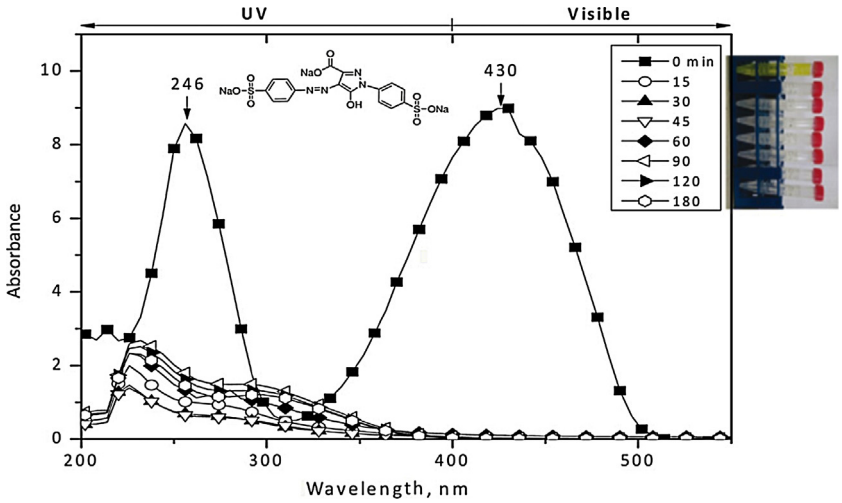

Fig. 5. The UV-vis spectra of E102 degradation process at different radiation times for the following experimental conditions: initial dye concentration = 200 mg/L; H_2O_2 = 1.75 mL/L; Fe^{2+} = 1.0 mM, pH = 3, temperature = 25 °C; UV wavelength = 365 nm; reaction time = 3 h.

the •OH by the ion excess. In this work, no significant change in %DCOD was detected in the studied range of Fe^{2+} concentration (not shown here). Therefore, a 1.0 mM Fe^{2+} concentration was selected for the final experimental design. This value is consistent with those reported elsewhere [8,29].

Recently, Oancea and Meltzer [30] have reported on the photo-Fenton efficiency in yellow 5 degradation. After 20 min of irradiation, (initial tartrazine concentration = 5.5 ppm, Fe^{2+} = 0.0828 mM, H_2O_2 = 0.062 mL/L), 98% of degradation was obtained and the decrease in TOC was up to 43%. The prolongation of the irradiation time (120 min) led only to the partial degradation of these small molecules and consequently TOC did not exceed 80% [31]. In this work, 100% of dye degradation, 99% of COD degradation and 85% of mineralization (TOC) were reached in 180 min. We believe that the observed discrepancies in the obtained results can be related to the difference between the initial dye concentration, reactor type and concentration of the oxidizing agent used. Gupta et al. [27] have studied the removal of tartrazine by photodegradation on titanium oxide (TiO_2 0.18 g/L and pH 11, UV lamp wavelength of 254 nm – heterogeneous photo-Fenton process). They have found that the photodegradation rate decreases with increasing dye concentration (from 10 to 32 ppm) and then it became almost constant up to 42 ppm. The increase in dye concentration from 10 to 42 ppm led to the decrease in the degradation efficiency from 96.12% to 41.89%, during 40 min of reaction. They found that TiO_2 concentration, light intensity and H_2O_2 concentration were the main factors that affected the decolorization process. The authors concluded that the maximum degradation efficiency was achieved with the combination of UV + H_2O_2 + TiO_2 (H_2O_2 1.5 mM) [30]. On the other hand, Thiama et al. [31] have investigated a traditional technology such as electrocoagulation (EC) and some emerging ones like electrochemical advanced oxidation processes (EAOPs). After 15 min of the treatment, the dye (278 ppm) degradation reached 100% and 60% TOC.

3.3. Mineralization study

In order to evaluate appropriately the degradation level that can be reached using the photo-Fenton process, it is necessary to understand the details of E102 dye mineralization. Fig. 6 presents the degradation percentages of COD and TOC achieved in this study.

As it could be seen, the change in COD degradation is more significant than that of TOC. It could be related to the fact that, in the earlier stages of wastewater oxidation, some partially oxidized intermediate compounds can be formed, which are unable to absorb UV radiation. As the process runs, the created intermediate compounds increase their oxidation state, finally achieving their partial mineralization. This suggests that oxidation would preferably occur on the chromophore structure rather than on the dye molecule skeleton. We believe that in the case of yellow 5 degradation, the •OH radicals can react by hydrogen abstraction from or addition to double bonds [32]. Thus, the •OH radicals first attack the azo groups and open the N = N bonds, destructing the long conjugated π systems, causing decolorization. Considering that C–C and C = C bonds, present in the aromatic ring structures, are stronger than N = N bonds, ring opening needs more time [33]. Consequently, the aromatic fragments remaining after the oxidation process can be considered as intermediate compounds. Under optimized conditions, a kinetic analysis was developed by monitoring %DCOD and %DTOC as a function of time. All experiments were performed during 180 min, at pH = 3, and at 25 °C. It was found that %DCOD dye degradation reached 99.8% at an initial dye concentration equal to 100 ppm (Fig. 4). The correlation between $\ln(C_i/C_{i0})$ and the irradiation time was linear, as in the case of a typical first-order plot [34]. The kinetic constant equaled 0.0791 min^{-1} (R^2 = 0.952).

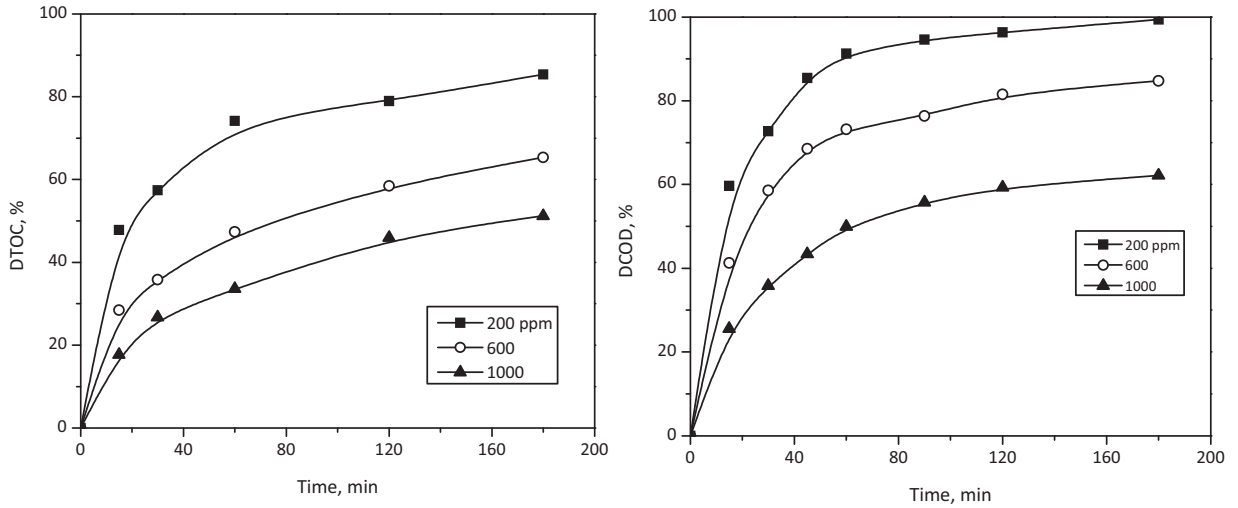

Fig. 6. The evolution of the TOC and the COD degradation percentages of wastewater treated using photo-Fenton process under the following experimental conditions: initial dye concentration = 200, 600, and 1000 ppm; H_2O_2 = 1.75 mL/L; Fe^{2+} = 1.0 mM, pH = 3, temperature = 25 °C; UV wavelength = 365 nm (4 W, one lamp).

3.4. Effect of the presence of inorganic ions

The presence of inorganic anions in textile wastewaters plays an important role in the photo-oxidation kinetics of different dyes. Some of them (e.g., the Cl^- anion) may be added to facilitate the dyeing process. However, the inorganic anions may induce or reduce the rate of photooxidation. It has been reported that the "common ion effect" due to the presence of inorganic anions led to a decreased π-electron (electrostatic) repulsion between two ionic dyes, increasing the degree of aggregation [35]. It is known that solubilization and ionization of dyes, which affect their attack by •OH radicals, decreased by increasing the aggregation degree. Thus the tendency for reaction between •OH radicals and the dye is expected to decrease as the dye undergoes greater aggregation [36]. A series of experiments were performed to study the effect of sodium chloride (NaCl), with concentrations similar to those of the operational conditions, on the photodegradation process. Fig. 7 presents the effect of NaCl on %DCOD during the photo-Fenton process.

One can see that %DCOD decreased dramatically in the presence of NaCl. This behavior may be attributed to •OH radical scavenging by the Cl^- ion, which is known to react with the •OH radical (forming an $OHCl^{\bullet -}$ radical) at pH 2–3 [37]. The $OHCl^{\bullet -}$ radical generated is less reactive than the •OH one, leading to a lower degradation rate of yellow 5 dye.

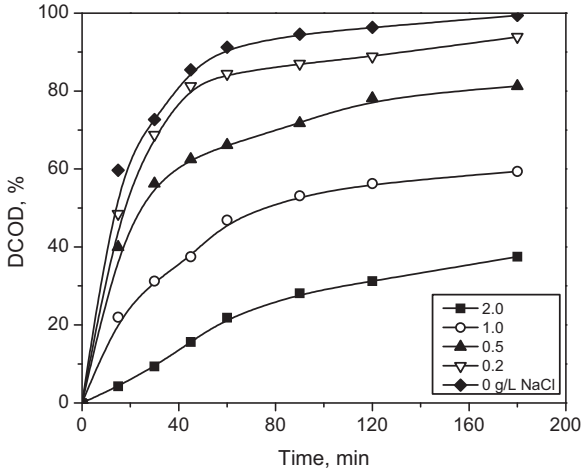

Fig. 7. Effect of NaCl concentration on the COD degradation percentages of wastewater treated by photo-Fenton process under the following experimental conditions: initial dye concentration = 200 ppm; H_2O_2 = 1.75 mL/L, Fe^{2+} = 1.0 mM, pH = 3, temperature = 25 °C; UV wavelength =365 nm (4 W, one lamp).

4. Conclusions

This study was focused on the optimization and implementation of a homogeneous photo-Fenton process for the decolorization and mineralization of a wastewater containing highly concentrated yellow 5 (E102) dye, resulting from an industry placed in the suburbs of Medellin (Colombia). The RSM was applied as a tool for the optimization of the operational conditions such as initial dyestuff concentration, H_2O_2 concentration, and UV-radiation power (number of lamps). The most significant results of the study can be summarized as follows:

- the following conditions were found to be optimal for decolorization and mineralization of yellow 5: UV radiation of 365 nm (4 W, one lamp), dye concentration of 200 mg/L, Fe^{2+} concentration of 1.0 mM, H_2O_2 concentration of 1.75 mL/L, treatment time of 180 min, Fe^{2+} concentration of 1 mM and pH = 3. Under these conditions, the photo-Fenton process allowed us to reach

ca. 100% of color dye degradation, 99% of COD degradation and 85% of mineralization (TOC);
- by increasing yellow 5 concentration (600 mg/L), 100% of color degradation, 80% of COD degradation and 60% of mineralization (TOC) were achieved, confirming the high efficiency of the proposed method for the solution containing a high dye concentration;
- COD removal was inhibited by the presence of the chloride anion, which produced an increase in the dye half-life from 90 to 540 min;
- the optimized and implemented UV/Fe^{+2}/H_2O_2 process can find a practical application in the purification of textile industrial wastewater developed at a large scale.

Acknowledgements

The authors thank to the "Dirección de Investigación de la Universidad EAFIT, Medellin", Colombia for financial support of this research. The staff of the "Laboratorio de Ingeniería de Procesos" is also recognized for their participation.

References

[1] M. Karkmaz, E. Puzenat, C. Guillard, J.M. Herrmann, Appl. Catal. B: Environ. 51 (2004) 183.
[2] M. Kobya, O. Taner, M. Bayramoglu, J. Hazard. Mater. 100 (2003) 163.
[3] M. Wawrkzkiewics, Z. Hubicki, J. Hazard. Mater. 164 (2009) 502.
[4] P. Bankovic, A. Milutinovic-Nikolic, Z. Mojovic, N. Jvic-Jovicic, M. Zunic, V. Dondur, Appl. Clay Sci. 58 (2012) 73.
[5] C. Lizama, J. Freer, J. Baeza, H.D. Mansilla, Catal. Today 76 (2002) 235.
[6] P. Carneiro, M. Osugi, C. Fugivara, N. Boralle, M. Furlan, M. Valnice, B. Zanoni, Chemosphere 59 (2005) 431.
[7] T.H. Kim, C. Park, E.B. Shin, S. Kim, Desalination 150 (2002) 165.
[8] E. GilPavas, M.Á. Gómez-García, Water Sci. Technol. 59 (2009) 1361.
[9] S.F. Kang, C.H. Liao, S.T. Po, Chemosphere 41 (2000) 1287.
[10] S. Malato, J. Blanco, M. Maldonado, I. Oller, W. Gernjak, L. Pérez, J. Hazard. Mater. 146 (2007) 440.
[11] X. Feng, S. Zhu, H. Hou, Environ. Technol. 27 (2006) 119.
[12] J. Feng, X. Hu, P.L. Yue, Chem. Eng. J. 100 (2004) 159.
[13] N. Modirshahla, M.A. Behnajady, F. Ghanbary, Dyes Pigment 73 (2007) 305.
[14] Y.H. Huang, Y.F. Huang, P.S. Chang, C.Y. Chen, J. Hazard. Mater. 154 (2008) 655.
[15] R. Liu, H.M. Chiu, C.S. Shiau, R.Y. Yeh, Y.T. Hung, Dyes Pigment 73 (2007) 1.
[16] M.J. Hernández-Rodríguez, C. Fernández-Rodríguez, J.M. Doña-Rodríguez, O.M. González-Díaz, D. Zerbani, J. Pérez Peña, J. Environ. Chem. Eng. 2 (2014) 163.
[17] C. Amor, E. De Torres-Socías, J.A. Peres, M.I. Maldonado, I. Oller, S. Malato, M.S. Lucas, J. Hazard. Mater. 286 (2015) 261.
[18] R. Sridhar, V. Sivakumar, V.P. Immanuel, J. Prakash, Environ. Prog. Sustain. Energy 31 (2012) 558.
[19] E. GilPavas, J. Medina, I. Dobrosz-Gómez, M.Á. Gómez-García, J. Appl. Electrochem. 44 (2014) 1421.
[20] D. Montgomery, Design and analysis of experiments, 5th Edition, Wiley and Sons, 2005.
[21] E. GilPavas, I. Dobrosz-Gómez, M.Á. Gómez-García, Water Sci. Technol. 65 (2012) 1795.
[22] S. Papić, D. Vujević, N. Koprivanac, D.L. Šinko, J. Hazard. Mater. 164 (2009) 1137.
[23] G. Centi, S. Perathoner, T. Torre, M.G. Verduna, Catal. Today 55 (1–2) (2000) 61–69.
[24] H. Shemer, Y.K. Kunukcu, K.G. Linden, Chemosphere 63 (2006) 269.
[25] Standard methods for the examination of water and wastewater, 20th edition (Centennial edition), American Public Health Association (APHA), Washington, DC, 2005.
[26] A.R. Khataee, A. Naseri, M. Zarei, M. Safarpour, L. Moradkhannejhad, Environ. Technol. 33 (2012) 1.
[27] V.K. Gupta, R. Jain, A. Nayak, S. Agarwal, M. Shrivastava, Mat. Sci. Eng. C 31 (2011) 1062.
[28] G. Buitrón, D. Prato-García, J. Hazard. Mater. 217 (2012) 293.
[29] R. Liu, H.M. Chiu, C.S. Shiau, R. Yu-Li Yeh, Y.T. Hung, Dyes Pigment 73 (2007) 1.
[30] P. Oancea, V. Meltzer, J. Taiwan Inst. Chem. Eng. 44 (6) (2013) 990–994.
[31] A. Thiama, M. Zhou, E. Brillas, I. Sirés, Appl. Catal. B: Environ. 150–151 (2014) 116.
[32] F.J. Benitez, J. Beltrán-Heredia, J.L. Acero, F.J. Rubio, Chemosphere 41 (2000) 1271.
[33] T. Ramesh, K. Tae Ouk, J. Jung Chul, B. Subramanian, M. Manickam, M. Il Shik, J. Hazard. Mater. 142 (2007) 308.
[34] H.S. Fogler, Elements of chemical reaction engineering, 4th Ed., Prentice Hall, NJ, USA, 2006.
[35] T.M. Elmorsi, Y.M. Riyad, Z.H. Mohamed, H.M. El Bary, J. Hazard. Mater. 174 (2010) 352.
[36] K. Ko, J. Lee, Y. Yoon, T. Moon, Y.H. Ahn, C.G. Park, K.S. Min, J.H. Park, Desalination Water Treat. 2 (2009) 6.
[37] D. Green, R. Perry, Perry's chemical engineers handbook, 8th Edition, McGraw-Hill, New York, 2008.